UNCERTAINTY AND SENSITIVITY OF ALTERNATIVE RN-222 FLUX DENSITY MODELS USED IN PERFORMANCE ASSESSMENT

G. J. Shott, V. Yucel, L. Desotell
National Security Technologies LLC
MS NSF-083, P.O. Box 98521, Las Vegas, NV 89521

G. Pyles, J. Carilli
National Nuclear Security Administration
Nevada Site Office, Las Vegas, NV 89030

ABSTRACT

Performance assessments for the Area 5 Radioactive Waste Management Site on the Nevada Test Site have used three different mathematical models to estimate Rn-222 flux density. This study describes the performance, uncertainty, and sensitivity of the three models which include the U.S. Nuclear Regulatory Commission Regulatory Guide 3.64 analytical method and two numerical methods. The uncertainty of each model was determined by Monte Carlo simulation using Latin hypercube sampling. The global sensitivity was investigated using Morris' one-at-a-time screening method, sample-based correlation and regression methods, the variance-based extended Fourier amplitude sensitivity test, and Sobol's sensitivity indices. The models were found to produce similar estimates of the mean and median flux density, but to have different uncertainties and sensitivities. When the Rn-222 effective diffusion coefficient was estimated using five different published predictive models, the radon flux density models were found to be most sensitive to the effective diffusion coefficient model selected, the emanation coefficient, and the radionuclide inventory. Using a site-specific measured effective diffusion coefficient significantly reduced the output uncertainty. When a site-specific effective-diffusion coefficient was used, the models were most sensitive to the emanation coefficient and the radionuclide inventory.

INTRODUCTION

Mathematical models are widely used to assess the long-term safety of radioactive waste disposal sites. Model results can have considerable uncertainty resulting from a lack of knowledge about what transport processes are important, the correct mathematical description of the transport processes, model input parameters, and the future state of the waste-disposal system. Uncertainty analysis provides decision makers with an understanding of the probability of decision errors. When the probability of decision errors is unacceptable, sensitivity analysis can identify the input parameters having the greatest impact on model output uncertainty. Further investigation of sensitive parameters may support a reduction in input parameter uncertainty, leading to a reduction in model output uncertainty. Sensitivity analysis can also identify unimportant model components and parameters that may allow model simplification. Uncertainty and sensitivity analyses are essential tools when mathematical models are used to guide decisions regarding management of radioactive waste disposal systems.

The radioactive decay of Ra-226 and its parents in low-level waste leads to the emission of gaseous Rn-222 and its progeny to the atmosphere, where exposure of the public may be a concern. Most regulatory agencies protect the public by limiting the Rn-222 flux density to 0.74 Bq m^{-2} s^{-1} over the surface of disposal units containing uranium ore residues [1, 2, 3]. Operators of disposal facilities typically control emissions by installing a low permeability cover, allowing radioactive decay of short-lived Rn-222 ($t_{½}$ = 3.8 d) to occur in the cover before reaching the atmosphere. The Rn-222 flux is reduced by selecting an appropriate cover thickness based on the gas permeability of the selected cover materials. This paper describes the results, uncertainty, and sensitivity of three alternative Rn-222 flux density models used in performance assessment at the Nevada Test Site (NTS).

MATERIALS AND METHODS

According to Fick's law of gaseous diffusion, the gas flux density is equal to the product of a proportionality constant known as the diffusion coefficient and the concentration gradient. In a porous medium, the diffusion coefficient must be adjusted to account for the reduced area available for diffusion and the longer path length in the air-filled pore space. Unfortunately there is no consistent way to write Fick's law for porous media. One common form is:

$$J = - D_e \, \phi \, \nabla C_a \qquad \text{(Eq. 1)}$$

where J is the flux per total area of medium (Bq m^{-2} porous medium s^{-1}), D_e is the effective diffusion coefficient in the porous medium (m^2 porous medium s^{-1}), ϕ is the total porosity (m^3 air m^{-3} porous medium), ∇ is the gradient operator (m^{-1} porous medium), and C_a is the Rn-222 concentration in the air-filled pore space (Bq m^{-3} air).

Radon-222 Flux Density Models

Starting with similar conceptual models, performance assessment modelers at the NTS have implemented three different mathematical models to estimate Rn-222 flux density. The first method is a widely used model developed by the U.S. Nuclear Regulatory Commission (NRC) for uranium mill tailings in Regulatory Guide 3.64 [4, 5]. The NTS implementation (denoted as *NRC model*) uses equation 12 in NRC Regulatory Guide 3.64, an analytical solution to a steady state one dimensional multiphase radon transport equation. The only difference between the *NRC model* the Regulatory Guide 3.64 model is that the Ra-226 activity concentration in waste is calculated as a function of time based on the initial concentration of U-234, Th-230, and Ra-226 in the former.

The other two models use numerical methods to obtain a transient solution to a series of coupled differential equations that are mass balance expressions for the multiphase transport of radon and its parents. The conceptual model of radionuclide transport at the Area 5 Radioactive Waste Management Site (RWMS) on the NTS assumes that there is no groundwater pathway and that all transport processes move radionuclides upwards to the ground surface. The most important difference between the numerical methods and the *NRC model* is that the former include upward transport processes for Rn-222 parents. The first numerical model was developed for a Title 40, Code of Federal Regulations, Part 191, performance assessment for transuranic wastes in Greater Confinement Disposal (GCD) Boreholes and is described as the *GCD model* throughout [6]. The second numerical model was implemented in the probabilistic simulation software GoldSim® for

low-level waste performance assessment and is referred to as the *GoldSim® model* [7]. The *GCD model* and the *NRC model* were implemented in Microsoft® Visual C++. Radon transport is multiphase in the *NRC* and *GoldSim models*, but limited to the gas phase in the *GCD model*. The processes included in each model are summarized in Table I.

Table I. Summary of processes assumed to contribute to the transport of Rn-222 in the three flux density models.

Process	***NRC Model***	***GoldSim® Model***	***GCD Model***
Radon Transport Processes			
Radioactive decay	X	X	X
Radon emanation from solid phase	X	X	
Radon emanation from liquid phase	X		
Radon adsorption on solid phase	X		
Radon dissolution in liquid phase	X	X	
Radon diffusion in the gas phase	X	X	X
Radon Parent Transport Processes			
Radioactive decay and ingrowth	X	X	X
Upward liquid advection		X	X
Diffusion in the liquid phase		X	X
Solution/Dissolution in liquid phase		X	X
Adsorption on the solid phase		X	X
Plant uptake and translocation		X	X
Invertebrate burrowing		X	X
Vertebrate burrowing		X	X

Rn-222 Effective Diffusion Coefficient

Estimating the Rn-222 flux density requires the effective diffusion coefficient. The Rn-222 effective diffusion coefficient can be obtained from predictive models or by direct measurement. Predictive models using porosity and water content as the independent variables are the simplest alternative, but questions about the universal applicability of these models persist [8]. Measurement of the effective diffusion coefficient offers the advantage of matching field multiphase conditions, but is time consuming and costly [9]. Transient and steady state laboratory measurement methods and field methods have been reported [10, 11, 12], but no standard methods are available, few laboratories have the equipment and expertise, and no standard reference materials or laboratory intercomparison programs exist.

Therefore, the *NRC* and *GCD models* were initially prepared using five alternative Rn-222 effective diffusion coefficient predictive models. Published models that were commonly used for Rn-222 or that were tested for a significant number of different soil types were selected. During the Monte Carlo simulations, a single diffusion coefficient model is selected at random by a model pointer and a diffusion coefficient estimated for that realization.

Nuclear Regulatory Commission Regulatory Guide 3.64 recommends that licensees use an empirical relationship for the effective diffusion coefficient of the form:

$$D_e = 7\ x\ 10^{-6}\ e^{\left[-4\left(S - S\phi^2 + S^5\right)\right]} \qquad \text{(Eq. 2)}$$

where D_e is the effective diffusion coefficient (m^2 porous medium s^{-1}), S is the moisture saturation of the medium (dimensionless), and ϕ is the total porosity (m^3 m^{-3}) [4]. Rogers and Nielson [9] later updated this relationship using over 1,000 measurements on soils. They recommended a relationship of the form:

$$D_e = D_o \, \phi \, e^{\left(-6\,S\,\phi - 6\,S^{14\,\phi}\right)} \qquad \text{(Eq. 3)}$$

where D_o is the ^{222}Rn free air diffusion coefficient (m^2 air s^{-1}).

Predictive models for the effective diffusion coefficient not specific to ^{222}Rn have been published in the soil physics literature. Jin and Jury [8] evaluated the validity of four published models and concluded that the model that best fit the data was the Millington and Quirk model [13]:

$$D_p = \frac{\varepsilon^2}{\phi^{2/3}} D_o \qquad \text{(Eq. 4)}$$

where D_p is the soil-gas diffusion coefficient (m^3 soil air m^{-1} soil s^{-1}), and ε is the air-filled porosity (m^3 m^{-3}). The soil-gas diffusion coefficient is assumed to be related to the effective diffusion coefficient as $D_e = D_p / \varepsilon$. Muldrup et al. [14] compared published models for dry sieved packed soil columns with measurements on wet soils. They proposed adjusting the dry soil models with a water-induced linear reduction (WLR) term, equal to the air-filled porosity divided by the total porosity (ε / ϕ), to account for moisture effects on the air-filled pore shape and connectivity. A WLR model based on a model described by Marshall [15]:

$$D_p = \frac{\varepsilon^{2.5}}{\phi} D_o \qquad \text{(Eq. 5)}$$

was found to best fit the data for six differently textured wet soils repacked in columns.

Muldrup et al. [16] have proposed and tested [17] a soil-water-characteristic (SWC) dependent model for undisturbed soils. Using data for 126 different soils, they found a high correlation between the macroporosity, ε_{100}, or porosity at a water potential of -100 cm H_20, and the diffusion coefficient. Substituting this relationship into a previously described expression for the unsaturated hydraulic conductivity modified for gas diffusivity, they obtained an expression of the form:

$$D_p = D_0 \, \left(2\,\varepsilon_{100}^3 + 0.04\,\varepsilon_{100}\right)\left(\frac{\varepsilon}{\varepsilon_{100}}\right)^{2+3/b} \qquad \text{(Eq. 6)}$$

where b is the Campbell [18] soil water retention parameter. The relationship between water potential and volumetric water content was measured by pressure plate apparatus [19] and thermocouple psychrometry [20] for 33 site samples. The Campbell [18] b parameter was calculated as the slope of the log-log transformed plot of 33 water potential and volumetric water content curves.

The site-specific effective diffusion coefficient was also estimated by laboratory measurement. A single alluvial sediment sample was collected as a composite of 10 randomly selected samples from stockpiled soils used for cover construction at the Area 5 RWMS. The random samples were collected from the soil pile surface by spade and sieved in the field through a 19 mm sieve. Samples were passed through a #4 sieve in the laboratory and packed in columns to the field-dry bulk density of 1.60 g cm^{-3}. Six replicate samples were prepared at four volumetric water contents, 0.05, 0.10, 0.15, and 0.20. The radon diffusion coefficient was measured using the

laboratory transient-diffusion method of Kalkwarf et al. [10]. The data were fit to a probabilistic linear model:

$$D_e = \beta\, \theta_{v\,c} + \alpha \qquad \text{(Eq. 7)}$$

where β and α are normally distributed variates and θ_v is the volumetric water content ($m^3\ m^{-3}$).

Uncertainty Analysis

A one-dimensional parameter uncertainty analysis was performed by assigning probability density functions (pdfs) to each input parameter, repeatedly sampling input pdfs using Latin hypercube sampling (LHS), and calculating model outputs. Uncertainty is defined here as the lack of knowledge about the mean conditions expected over the dimensions and the design life of the disposal facility. Therefore, the observed variability in input parameters (i.e., real spatial and temporal differences in the population) does not appropriately describe the desired pdf. The long-term spatial and temporal mean conditions where represented by using the mean and standard error of the data when site-specific data were available. Model inputs are summarized in Table II.

Table II. Input parameter distributions

Model[a]	Parameter (units)	Distribution(parameter values)[b]
1pm, 2pm	U-234 half-life (yrs)	Triangular (2.455, 2.461, 2.449 x 10^5)
1pm, 2pm	Th-230 half-life (yrs)	Triangular (7.588, 7.618, 7.558 x 10^4)
1pm, 2pm	Ra-226 half-life (yrs)	Triangular (1,600, 1,607, 1,593)
2pm	Longitudinal dispersivity (m)	Uniform (0.01, 0.3)
2pm, 3	Liquid advection rate (m yr^{-1})	Beta (0.751, 1.78, 6.55E-7, 5.40E-4)
2pm, 3	Liquid diffusion coefficient ($m^2\ yr^{-1}$)	Uniform (0.0095, 0.0631)
3	Ostwald Rn solubility coefficient	Triangular (0.25, 0.26, 0.24)
1pm, 2pm, 3	Dry bulk density (g cm^{-3})	Normal (1.59, 0.01)
1pm, 2pm, 3	Particle density (g cm^{-3})	Normal (2.54, 0.01)
2pm, 3	Depth of no liquid water flux boundary (NFB) (m)	Triangular (2, 1.5, 2.5)
3	Volumetric water content above NFB ($m^3\ m^{-3}$)	Normal (0.0577, 0.0002)
2pm, 3	Volumetric water content below NFB ($m^3\ m^{-3}$)	Normal (0.079, 0.001)
1p, 2p, 3	Rn-222 free air diffusion coefficient ($m^2\ s^{-1}$)	Uniform (1.0 x 10^{-5}, 1.2 x 10^{-5})
1m, 2m, 3	Rn-222 D_e coefficient regression slope	Normal (-1.699 x 10^{-5}, 1.94 x 10^{-6})
1m, 2m, 3	Rn-222 D_e coefficient regression intercept	Normal (4.99 x 10^{-6}, 2.64 x 10^{-7})
1p, 2p	Cover Campbell b water retention parameter	Normal (4.3, 0.1)
1p, 2p	Cover macroporosity ($m^3\ m^{-3}$)	Normal (0.146, 0.006)
1pm, 2pm, 3	Initial Ra-226 waste concentration (Bq m^{-3})	Lognormal (1.9 x 10^5, 1.63)
1pm, 2pm, 3	Initial Th-230 waste concentration (Bq m^{-3})	Lognormal (6.0 x 10^5, 1.70)
1pm, 2pm, 3	Initial U-234 waste activity concentration (Bq m^{-3})	Lognormal (2.0 x 10^8, 1.43)
1pm, 3	Waste emanation coefficient	Normal (0.02, 0.8)
2pm, 3	U-234 plant concentration ratio	Lognormal (0.017, 5.7)
2pm, 3	Th-230 plant concentration ratio	Lognormal (6.6E-3, 5.7)
2pm, 3	Ra-226 plant concentration ratio	Lognormal (0.075, 5.7)
2pm, 3	U-234 distribution coefficient ($m^3\ kg^{-1}$)	Lognormal (7.2E-3, 1.60)
2pm, 3	Th-230 distribution coefficient ($m^3\ kg^{-1}$)	Lognormal (6.3, 1.58)
2pm, 3	Ra-226 distribution coefficient ($m^3\ kg^{-1}$)	Uniform (0.07, 0.3)
2pm, 3	U-234 solubility constant (moles L^{-1})	Uniform (2E-6, 7E-3)
2pm, 3	Th-230 solubility constant (moles L^{-1})	Uniform (6E-8, 6E-6)
2pm, 3	Ra-226 solubility constant (moles L^{-1})	Loguniform (9E-9, 9E-7)
2pm, 3	Annual grasses primary productivity (kg $m^{-2}\ yr^{-1}$)	Normal (6.2E-4, 2.2E-4)

Model[a]	Parameter (units)	Distribution(parameter values)[b]
2pm, 3	Annual grasses root to shoot ratio	Triangular (1.53, 2, 1)
2pm, 3	Perennial primary productivity (kg m^{-2} yr^{-1})	Normal (7.35E-2, 8.6E-3)
2pm, 3	Shrub primary productivity (kg m^{-2} yr^{-1})	Normal (0.22, 0.026)
2pm, 3	Annual grasses root distribution parameter	Normal (2.19, 0.036)
2pm, 3	Perennial root distribution parameter	Normal (23.9, 0.313)
2pm, 3	Shrub root distribution parameter	Normal (14.6, 0.0807
2pm, 3	Annual grasses root depth (m)	Normal (1.58, 0.50)
2pm, 3	Perennial root depth (m)	Normal (3.6, 0.9)
2pm, 3	Shrub root depth (m)	Normal (3.15, 0.79)
2pm, 3	Invertebrate burrowing rate (kg m^{-2} y-1)	Normal (0.22, 0.05)
2pm, 3	Invertebrate burrow depth (m)	Normal (3.3, 1.2)
3	Pogonomymex sp. nest volume (m^3)	Normal (0.64, 0.09)
3	Pogonomymex sp. colony life span (yrs)	Normal (20.2, 3.6)
3	Pogonomymex sp. colony density (ha^{-1})	Normal (28, 4)
3	Pogonomymex sp. burrow shape parameter	Normal (10, 0.71)
3	Messor sp. nest volume (m^3)	Normal (0.94, 0.26)
3	Messor sp. colony life span (yrs)	Normal (9, 1.5)
3	Messor sp. colony density (ha^{-1})	Normal (4.7, 1.8)
3	Messor sp. burrow shape parameter	Normal (8.4, 1.5)
2pm, 3	Mammal burrowing rate (kg m2 y-1)	Normal (2.79, 0.70)
2pm, 3	Mammal burrow depth (m)	Normal (2.0, 0.5)
3	Rodent mound volume (m^3 yr^{-1})	Normal (0.092, 0.006)
3	Rodent mound density (ha^{-1})	Normal (192, 13.7)
3	Rodent burrow shape parameter	Normal (4.5, 0.84)
3	Large mammal mound volume (m^3 yr^{-1})	Normal (0.14, 0.04)
3	Large mammal mound density (ha^{-1})	Normal (2, 1.4)
3	Large mammal burrow shape parameter	Normal (4.7, 0.69)
3	Soil resuspension rate (yr^{-1})	Uniform (8 x10^{-6}, 1 x 10^{-3})
3	Wind speed (m s^{-1})	Normal (2.6, 0.09)

[a] – 1p – *NRC model* with predicted D_e, 1m – *NRC model* with measured D_e, 2p - *GCD model* with predicted D_e, 2m – *GCD Model* with measured D_e, 3 – *GoldSim® model* with measured D_e

[b] Triangular parameters: mode, maximum, minimum; normal parameters: mean, standard deviation; uniform parameters: minimum, maximum; lognormal parameters: geometric mean, geometric standard deviation; beta parameters: alpha, beta, minimum, maximum

Sensitivity Analysis

Sensitivity analyses were performed using SimLab 2.2 [21]. The one-at-a-time screening method of Morris [21, 22] was performed using eight replicates and a sample size of 344 and 136 for the *GCD* and *NRC models* with the predictive effective diffusion coefficient models and 328, 112, and 384 realizations for the *GCD, NRC*, and *GoldSim® models* using the measured site-specific effective diffusion coefficient. Sample-based methods were applied to model results for 4,000 realizations using LHS. Scatterplots, the Pearson product correlation coefficient (PEAR), standardized regression coefficient (SRC), and partial correlation coefficient (PCC) were generated for the raw data. The Spearman coefficient (SPEAR), standardized rank regression coefficient (SRRC), and the partial rank correlation coefficient (PRCC) were generated for the rank transformed data. Variance-based global sensitivity indices (SIs) were calculated using the extended Fourier amplitude sensitivity test (FAST) and Sobol's method. FAST and Sobol SIs were calculated with sample sizes ranging from 4k to 16k realizations.

RESULTS

The production of Rn-222 in waste at the Area 5 RWMS is expected to increase over time because the radon parent inventory proportions are currently U-234 > Th-230 > Ra-226. The results from the *GoldSim® model*, which shows the maximum Rn-222 flux density occurring at the end of the 1,000-year compliance period, is representative of all three models (Fig. 1).

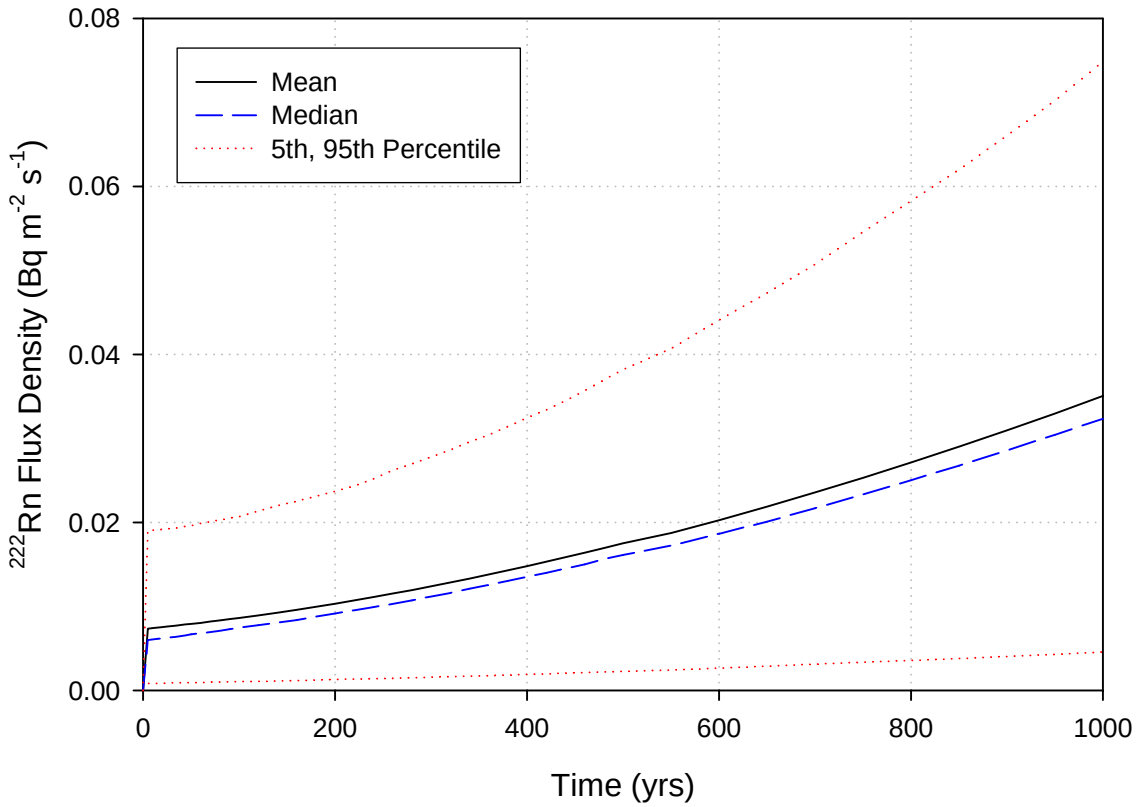

Fig. 1. Mean, median, 5th and 95th percentile Rn-222 flux density over time as estimated by the *GoldSim® model* from 4,000 realizations.

When the predictive models for Rn-222 effective diffusion coefficients were used, the *GCD model* produced slightly higher mean-flux density estimates than the *NRC model* (Fig 2). When the laboratory-measured effective diffusion coefficient was used, the *NRC* and *GoldSim® model* produced similar means, while the *GCD model* continued to give slightly higher results. The *GCD model* does not include an emanation coefficient, effectively assuming that all Rn-222 is released to the air-filled pore space. This may in part explain the higher Rn-222 flux densities estimated by the *GCD model*.

All models indicate a high expectation of compliance with the 0.74 Bq m^{-2} s^{-1} performance objective. The models using the predictive relationships for the effective diffusion coefficient show considerably higher uncertainty than the models using the measured effective diffusion coefficient. The *GCD model* shows the largest reduction in uncertainty with use of the

measured site-specific effective diffusion coefficient. The Rn-222 flux density distributions for the *NRC* and *GoldSim® models* are nearly identical.

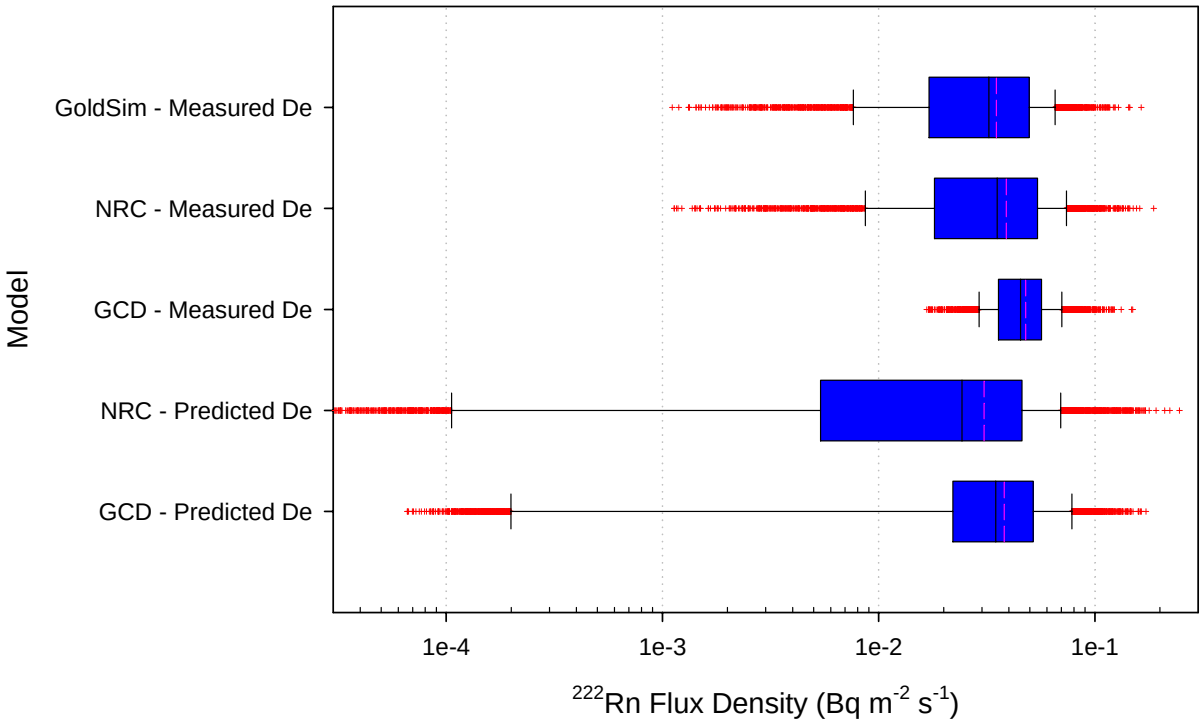

Fig. 2. Box plots of Rn-222 flux density at 1,000 years for five alternative models. Plot shows 10th, 25th, 50th, 75th, and 90th percentiles, mean (dashed) and outliers (cross hair).

Morris's one-at-a-time method is a global sensitivity method that identifies parameters with negligible effects, linear and additive effects, and nonlinear or interactive effects [21, 23]. The method calculates the mean and standard deviation of replicated local sensitivity measures. A mean value that is high relative to other parameters indicates linear and additive effects. A high standard deviation indicates nonlinear or interactive effects. Considering both the mean and standard deviation for the *NRC model* with the predictive effective diffusion coefficient models, sensitive parameters are the emanation coefficient, the effective diffusion coefficient model pointer, Th-230 inventory, U-234 inventory, the Rn-222 free air diffusion coefficient (D_o), and the Ra-226 inventory (Fig. 3). The only parameters showing potentially important nonlinear or interactive effects are the emanation coefficient and the effective diffusion coefficient model pointer. There is a nonmonotonic relationship between the value of the arbitrary model pointer and the effective diffusion coefficient, which probably explains the nonlinear or interactive effects for this parameter.

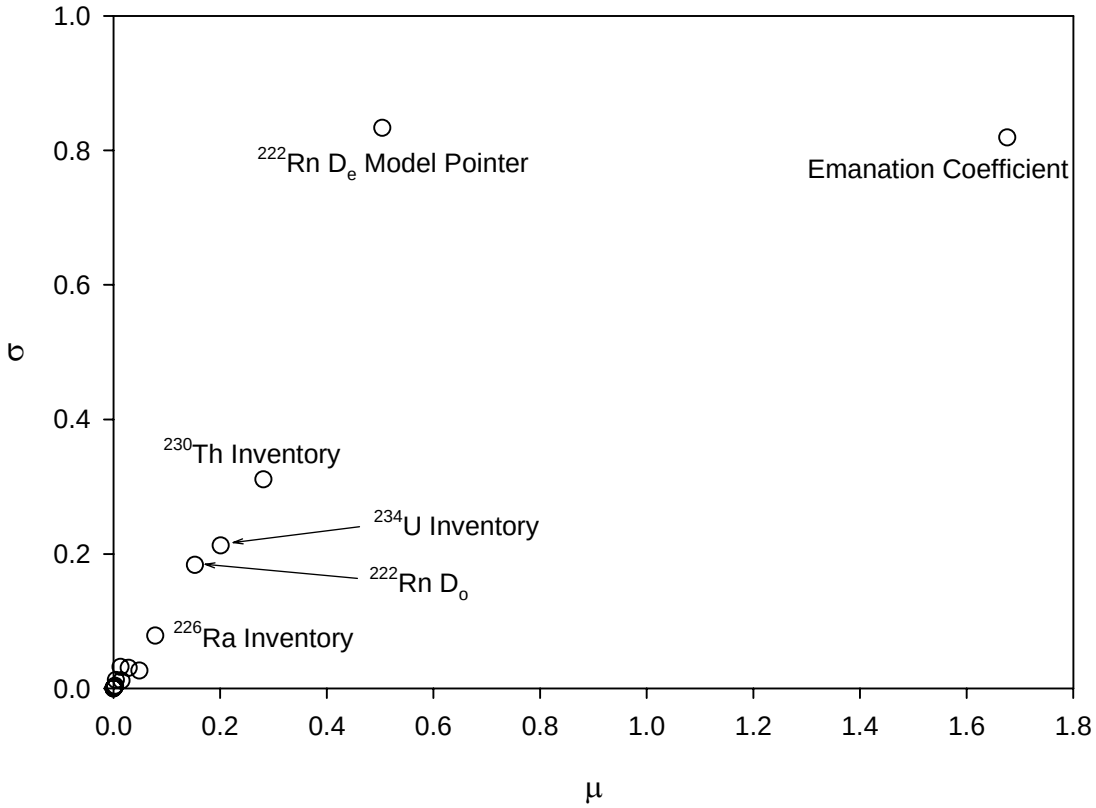

Fig. 3. Morris' one-at-a-time method mean and standard deviation for the *NRC model* with predicted Rn-222 effective diffusion coefficient.

Morris' method is very economical as the minimum sample size is r (k + 1) where r is the number of local sensitivity replicates and k is the number of model parameters. The *GoldSim® model*, with the largest number of parameters at 47, only requires 192 realizations for four replicates. However, experimentation with different numbers of replicates indicated that increasing the number of replicates increased the number of nonnegligible (i.e., sensitive) parameters and produced results more consistent with the results of other sensitivity measures discussed below. The final analysis was performed with eight replicates, which required less than 400 realizations for all models.

The *GCD model* with the predictive effective diffusion coefficient relationships showed similar sensitivities except that it does not include an emanation coefficient and showed slight sensitivity to two upward transport parameters: U solubility constant (K_{sp}) and the liquid diffusion coefficient (Table III).

Table III. Morris' screening method mean and standard deviation for the *GCD* and *NRC models* using five predictive models for the Rn-222 effective diffusion coefficient.

Parameter	***GCD Model*, Predicted D_e**		***NRC Model*, Predicted D_e**	
	Mean	**Standard Deviation**	**Mean**	**Standard Deviation**
Emanation Coefficient	a	a	1.68	0.819
D_e Model Pointer	0.761	0.880	0.504	0.833
U-234 Inventory	0.706	0.290	0.201	0.212
Th-230 Inventory	0.448	0.233	0.281	0.311
Ra-226 Inventory	0.220	0.183	0.078	0.078
Rn-222 Free Air D_o	0.258	0.176	0.153	0.183
U K_{sp}	0.190	0.316	a	a
Liquid Diffusion Coefficient	0.117	0.136	a	a
All others	<0.06	<0.03	<0.05	<0.03

a – parameter not in model

The models using the measured effective diffusion coefficient showed similar sensitivities (Table IV). In these models the effective diffusion coefficient model pointer is replaced by pdfs for the slope and intercept of the effective diffusion coefficient regression. These effective diffusion coefficient pdfs show reduced sensitivity compared to the predictive model pointer.

Table IV. Morris' screening method mean and standard deviation for the *GCD, NRC*, and *GoldSim® models* using a Rn-222 effective diffusion coefficient measured in the laboratory.

Parameter	***GCD Model*, Measured D_e**		***NRC Model*, Measured D_e**		***GoldSim® Model*, Measured D_e**	
	Mean	**Standard Deviation**	**Mean**	**Standard Deviation**	**Mean**	**Standard Deviation**
Emanation Coefficient	a	a	1.56	0.296	0.066	0.011
U-234 Inventory	0.669	0.212	0.502	0.272	0.025	0.015
Th-230 Inventory	0.491	0.243	0.420	0.301	0.021	0.015
Ra-226 Inventory	0.204	0.066	0.141	0.150	0.008	0.003
D_e Regression Slope	0.544	0.144	0.361	0.187	b	b
D_e Regression Intercept	0.312	0.109	0.192	0.121	b	b
U K_{sp}	0.182	0.286	a	a	<0.001	<0.001
Liquid Diffusion Coefficient	0.122	0.141	a	a	<0.001	<0.001
All others	<0.06	<0.06	<0.03	<0.02	<0.001	<0.001

a – parameter not in model
b – parameter fixed

Scatterplots, correlation, and regression analysis are convenient sensitivity methods because they use the same LHS sample used in uncertainty analysis. Examination of the scatterplots for the *GCD* and *NRC model* with predictive effective diffusion coefficient models showed no strong relationships between the flux density and input parameters except for the effective diffusion coefficient model pointer and for the emanation coefficient for the *NRC model* only. The *GCD model* does not include an emanation coefficient. The scatterplot for the effective diffusion coefficient model pointer clearly shows a nonmonotonic relationship. The *GCD* and *NRC model* with the predictive effective diffusion coefficient relationships are nonmonotonic. The *NRC*

model shows a positive linear relationship between flux density and the emanation coefficient and suggests that non-additive effects with other parameters are occurring.

The *GCD* and *NRC model* with predicted effective diffusion coefficients had five parameters with p-values less than 0.01 (Table V). The PEAR, SRC, and PCC all gave the same ranking for these parameters. The PEAR and SRC values are similar, as expected for an uncorrelated sample. The PCC is slightly higher than the PEAR and SRC. The coefficient of determination, R^2, for these two models is low, 0.24 for the GCD model and 0.43 for the *NRC model*, indicating that the PEAR, SRC, and PCC results are suspect for these models. Again, this is likely due to nonmonotonicity.

The sensitivity measures calculated for the rank transformed data, the SPEAR, SRRC, and PRCC, yielded less consistent parameter rankings. The rank transformation is expected to perform poorly with nonmonotonic data.

Table V. Parameter ranks from sample-based sensitivity measures for the *GCD* and *NRC models* using five predictive models for the Rn-222 effective diffusion coefficient.

Parameter	***GCD Model*, Predicted D_e**		***NRC Model*, Predicted D_e**	
	Raw Data (PEAR, SRC, PCC)	**Rank Data (SPEAR, SRRC, PRCC)**	**Raw Data (PEAR, SRC, PCC)**	**Rank Data (SPEAR, SRRC, PRCC)**
D_e Model Pointer	1 [a]	2 [a], 3 [a], 3	2 [a]	2 [a]
Emanation Coefficient	B	b	1 [a]	1 [a]
U-234 Inventory	2 [a]	1 [a]	3 [a]	2 [a]
Th-230 Inventory	3 [a]	10, 20, 20	4 [a]	4 [a]
Ra-226 Inventory	4 [a]	5 [a]	5 [a]	6, 7, 7
U-234 K_d	5	6	B	b
Rn-222 Free Air D_o	6	4 [a]	29, 36, 36	5 [a]

[a] – statistically significant, p-value < 0.01
b – parameter not in model

Examination of the scatterplots for the *GCD, NRC*, and *GoldSim® model* with measured diffusion coefficient models showed no strong relationships between the flux density and input parameters except for the emanation coefficient for the *NRC* and *GoldSim® models* only. The *NRC* and *GoldSim® models* show a positive linear relationship between flux density and the emanation coefficient and suggest that non-additive effects may be present (Fig. 4).

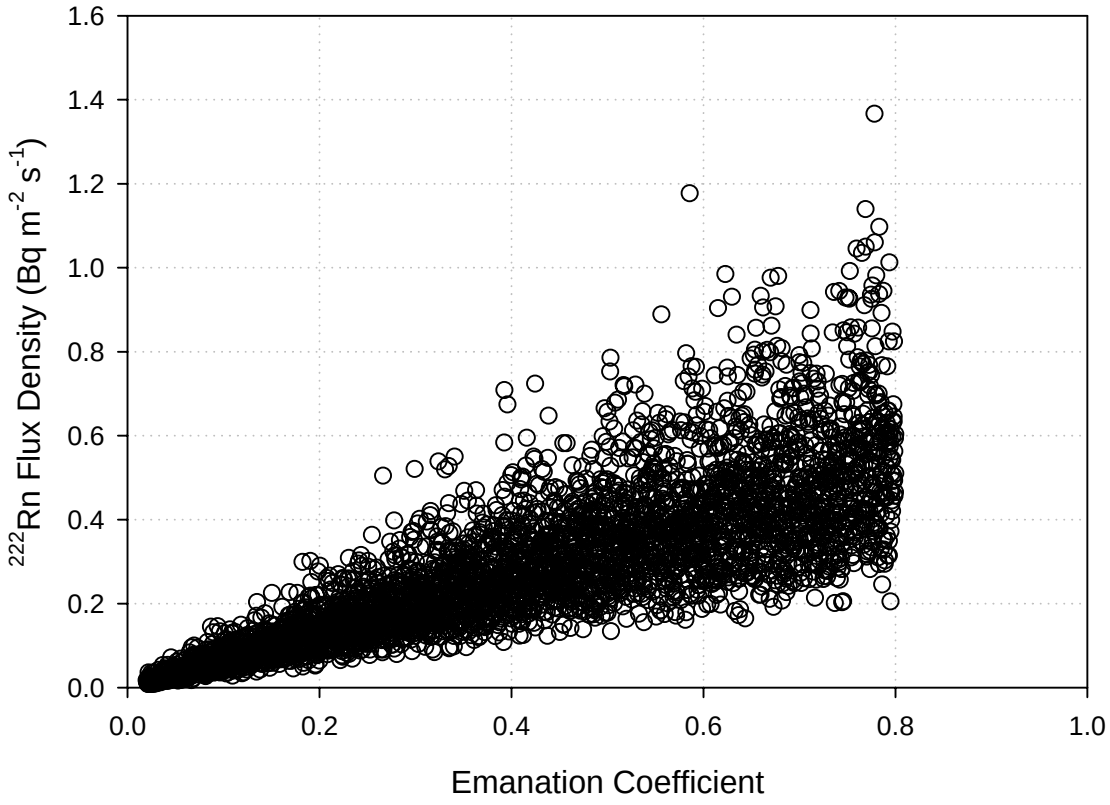

Fig. 4. Scatterplot of Rn-222 flux density versus emanation coefficient for the *GoldSim*® *model*.

The *GCD, NRC*, and *GoldSim*® *models* using the measured effective diffusion coefficient had four to seven parameters with p-values less than 0.01. The results for the raw data and ranked data gave the same rankings for at least the first four parameters (Table VI). The coefficients of determination, R^2, were high (0.95, 0.92, and 0.95) for the *GCD, NRC*, and *GoldSim*® *models* respectively, indicating that a linear model can account for most of the variability observed in the output. There was little or no improvement with the rank transform, confirming that these models are well represented by a linear model. The sensitivity measures calculated for the rank-transformed data, the SPEAR, SRRC, and PRCC, yielded consistent parameter rankings for statistically significant parameters.

Table VI. Parameter ranks from sample-based sensitivity measures for the *GCD, NRC*, and *GoldSim® models* using an Rn-222 effective diffusion coefficient measured in the laboratory.

Parameter	*GCD Model*, Measured D_e		*NRC Model*, Measured D_e		*GoldSim® Model*, Measured D_e	
	Raw Data (PEAR, SRC, PCC)	Rank Data (SPEAR, SRRC, PRCC)	Raw Data (PEAR, SRC, PCC)	Rank Data (SPEAR, SRRC, PRCC)	Raw Data (PEAR, SRC, PCC)	Rank Data (SPEAR, SRRC, PRCC)
Emanation Coefficient	c	c	1 [a]	1 [a]	1 [a]	1 [a]
U-234 Inventory	1 [a]	1 [a]	2 [a]	2 [a]	3 [a]	3 [a], 2 [a], 2
Th-230 Inventory	2 [a]	2 [a]	3 [a]	3 [a]	2 [a]	2 [a], 3 [a], 3
Ra-226 Inventory	5 [a]	5 [a]	6 [a]	6 [a]	4 [a]	4 [a]
D_e Regression Slope	3 [a]	3 [a]	4 [a]	4 [a]	b	b
D_e Regression Intercept	4 [a]	4 [a]	5 [a]	5 [a]	b	b
U-234 K_d	6 [a], 7 [a], 7	6 [a]	c	c	6, 31, 31	8, 46, 46
Ra-226 Plant Soil CR	13, 20, 21	24, 21, 21	c	c	5, 11, 11	7, 18, 18
Bulk Density	27, 19, 19	20, 34, 34	18, 11, 11	35, 27,27	18, 5, 5	24, 5, 5
Liquid Diffusion Coefficient	7 [a], 7 [a], 6	7 [a]	c	c	23, 8, 8	21, 6, 6

[a] – statistically significant, p-value < 0.01
b – parameter fixed
c – parameter not in model

The extended FAST and Sobol's sensitivity indices are variance decomposition methods that provide quantitative and model-independent estimates of the contribution of each input parameter to the variance observed in the output [22, 23, 24]. These methods can provide indices of first order effects and at greater computational effort, total effects. The sum of total effects for all parameters should be 1.0 and first order effects should be 1.0 or less. However, when the sample size is small, the sum of the total effects SI can be much greater than 1.0 and Sobol's SIs may be negative. The results of both methods should converge as the sample size increases.

First order SIs obtained with 4k and 16k realizations were similar and summed to a values less than 1.0 (Table VII). There is a significant difference between the FAST and Sobol's SIs and the differences were observed to decrease with increasing sample size. The total effects SIs summed to much greater than 1.0 even with greater than 16k realizations. Therefore, the total effects SIs were considered unusable.

The SIs for first order effects produced a ranking that is similar to the other tests. A majority of the variability in the *GCD model* with the predictive effective diffusion coefficient relationships (61 percent by FAST and 76 percent by Sobol's SI) are attributable to the diffusion coefficient model pointer. A majority of the *NRC model* first-order SI was divided between the effective diffusion coefficient model pointer and the emanation coefficient. From 77 to 92 percent of the output variability was attributable to first-order effects.

Increasing the sample size from 4k to more than 12k had a lesser effect on the *GCD, NRC*, and *GoldSim® models* using the measured effective diffusion coefficient. Usable total effect SIs could not be obtained with more than 12k realizations.

Table VII. Extended FAST and Sobol's first order SIs for the *GCD* and *NRC models* using five predictive models for the Rn-222 effective-diffusion coefficient.

Parameter	***GCD Model*, Predicted D_e**		***NRC Model*, Predicted D_e**	
	FAST SI (n = 16,171)	**Sobol SI (n = 16,384)**	**FAST SI (n = 16,171)**	**Sobol SI (n = 16,384)**
D_e Model Pointer	0.61	0.76	0.35	0.44
Emanation Coefficient	a	a	0.34	0.25
U-234 Inventory	0.08	0.08	0.04	0.04
Th-230 Inventory	0.04	0.06	0.05	0.04
Ra-226 Inventory	<0.01	< 0.01	<0.01	<0.01
Rn-222 Free Air D_o	0.02	0.01	<0.01	0.01
All others	0.02	0.01	0.02	<0.01
Total	0.77	0.92	0.81	0.77

a– parameter not in model

When the measured effective diffusion coefficient was used, first order effects were even more important, with from 91 to 100 percent of the output variability explained by first order effects (Table VIII). A majority of output variability was explained by variability in the emanation coefficient for the *NRC* and *GoldSim® model*. The *GCD model* which does not include an emanation coefficient was most sensitive to the radionuclide inventory. The Goldsim® multivariate result element can calculate a variance-based first order SI it calls an importance measure. The Goldsim® importance values are very similar to the Sobol's SI. The emanation coefficient, U-234 Inventory, and Th-230 inventory importance measures were 0.74, 0.08, and 0.08, respectively.

Table VIII. Extended FAST and Sobol's first order SIs for the *GCD, NRC*, and *GoldSim® models* using a Rn-222 effective diffusion coefficient measured in the laboratory.

Parameter	***GCD Model*, Measured D_e**		***NRC Model*, Measured D_e**		***GoldSim® Model*, Measured D_e**	
	FAST SI (n=13,482)	**Sobol SI (n=16,384)**	**FAST SI (n=13,482)**	**Sobol SI (n=16,384)**	**FAST SI (n=12,079)**	**Sobol SI (n=14,336)**
Emanation Coefficient	b	b	0.83	0.69	0.61	0.76
U-234 Inventory	0.47	0.36	0.09	0.09	0.15	0.09
Th-230 Inventory	0.22	0.32	0.09	0.08	0.09	0.10
Ra-226 Inventory	0.07	0.05	0.01	0.01	0.02	0.01
D_e Regression Slope	0.19	0.20	0.05	0.04	a	a
D_e Regression Intercept	0.07	0.07	0.01	0.02	a	a
Perennial Plants Root Shape Factor	0.02	<0.01	b	b	<0.01	<0.01
Liquid Diffusion Coefficient	0.01	<0.01	b	b	<0.01	<0.01
All others	0.07	0.01	0.03	0.01	0.04	<0.01
Total	1.10	1.01	1.11	0.94	0.91	0.96

a– parameter fixed
b– parameter not in model

DISCUSSION

All models evaluated produced similar mean and median Rn-222 flux density values. The uncertainty analysis of all five models, including the two models with predictive models for the Rn-222 effective diffusion coefficient, indicated a high probability of compliance. If the purpose of the uncertainty analysis was only to assess the likelihood of compliance, then further reduction in uncertainty by measurement of the site-specific effective diffusion coefficient is probably not warranted for this waste inventory. However, since the performance objectives also require that doses be maintained as low as reasonably achievable, an optimization process beyond simple compliance with a regulatory limit is implied. The main option available for reducing Rn-222 emissions is changing cover thickness. As cover construction costs are high, measurement of the site-specific effective diffusion coefficient was judged cost effective. Once uncertainty in the effective diffusion coefficient was reduced, model output uncertainty was controlled by the emanation coefficient and to a much lesser extent by the waste inventory. Further characterization of these wastes is not feasible, because the waste is already disposed and originated from many sources with multiple physical and chemical forms. Consequently, further reductions in model uncertainty are not likely to be obtained.

Although each of the applied global sensitivity analysis methods identified the same parameters as sensitive, and produced similar rankings, each had distinct advantages and disadvantages. The advantages of the Morris one-at-a-time screening method are its small sample size and model independence. Its disadvantages are that the results are qualitative and require judgment to distinguish the degree of linearity/nonlinearity in the relationship between inputs and outputs. It also uses a nonrandom input vector, thus requiring a separate experiment and a model that can read the input vectors. The advantage of the sample-based methods is that they can use the same LHS inputs and outputs as uncertainty analysis. The disadvantages arise in interpretation of results for models that are nonlinear or nonmonotonic. The variance-based techniques offer quantitative model-independent SIs. The disadvantages are that large sample sizes are required, especially to obtain higher or total order effects, and as for Morris' method, a nonrandom set of input vectors is required. The FAST method requires a smaller sample size than the Sobol's SIs. Sobol's method, however, has the capability to calculate higher-order effects, whereas extended FAST is limited to total effects. For the models evaluated here, reliable first-order SIs were obtained with as little as 4k realizations, but even 16k realizations were insufficient to determine total effect SIs.

CONCLUSIONS

Five alternative Rn-222 flux density models developed from similar conceptual models produced similar estimates of mean and median flux, but displayed different uncertainties and sensitivities. Using a site-specific Rn-222 effective diffusion coefficient measured in the laboratory rather than published predictive relationships significantly reduced uncertainty in the flux density at 1,000 years.

Morris's one-at-a-time screening method, sample-based methods, and variance-decomposition methods of sensitivity analysis produced similar rankings of sensitive parameters. For the case where site-specific Rn-222 effective diffusion coefficient was unknown, the models were most

sensitive to (in decreasing order of sensitivity), the effective-diffusion-coefficient model selected, the emanation coefficient, the U-234, Th-230, and the Ra-226 inventories. When the site-specific effective diffusion coefficient was available the models were most sensitive to (in decreasing order of sensitivity), the emanation coefficient, U-234, Th-230, and the Ra-226 inventory. The models were found to be insensitive to parameters describing upward transport processes for Ra-226 and its parents.

Each sensitivity method had its advantages and disadvantages. Selection of the most appropriate sensitivity method must be based on consideration of the model properties of linearity and monotonicity, computational expense, and the ability to process input samples generated externally by sensitivity analysis software.

REFERENCES

1. U.S. Department of Energy. Radioactive waste management manual, DOE M 435.1-1 Chg. 1 [online]. Available at: http://www.directives.doe.gov/cgi-bin/explhcgi?qry1511248156;doe-183. Accessed 22 November 2004.
2. U.S. Environmental Protection Agency. Title 40 – Protection of environment, Chapter 1—Environmental Protection Agency, Part 61 – National emission standards for hazardous air pollutants [online]. Available at: http://www.access.gpo.gov/nara/cfr/waisidx_99/40cfr61_99.html. Accessed 22 November 2004.
3. U.S. Nuclear Regulatory Commission. Part 40 – Domestic licensing of source material [Online]. Available at: http://www.nrc.gov/reading-rm/doc-collections/cfr/part040/. Accessed 22 November 2004.
4. U.S. Nuclear Regulatory Commission. Calculation of radon flux attenuation by earthen uranium mill tailings covers. Washington DC: U.S. Nuclear Regulatory Commission; Regulatory Guide 3.64; (1989).
5. Rogers, V. C., K. Nielson, Multiphase radon generation and transport in porous materials. Health Physics 61: 807-815; (1991).
6. Sandia National Laboratory. Compliance assessment document for the transuranic waste in the Greater Confinement Disposal Boreholes at the Nevada Test Site, Volume 2: Performance assessment. Albuquerque, NM: Sandia National Laboratory; (1999).
7. Bechtel Nevada, Neptune and Company. Addendum 2 to the performance assessment for the Area 5 Radioactive Waste Management Site at the Nevada Test Site, Nye County, Nevada. Las Vegas, NV: Bechtel Nevada, DOE/NV/11718—176-ADD2; (2006).
8. Jin Y., A. Jury, Characterizing the dependence of gas diffusion coefficient on soil properties. Soil Sci. Soc. Am. J. 60: 66-71; (1996).
9. Rogers, V. C, Nielson K. K. Correlations for predicating air pemeabilities and ^{222}Rn diffusion coefficients in soils. Health Physics 61: 225-230; (1991).
10. Kalkwarf, D. R., K. K. Nielson, D.C. Rich, V.C. Rogers. Comparison of radon diffusion coefficients measured by transient-diffusion and steady state laboratory methods. Washington DC: U.S. Nuclear Regulatory Commission, NUREG/CR-2875; November 1982.
11. Rolston, D. E.. Gas Diffusivity. In: Klute A, ed. Methods of soil analysis, Part 1, Physical and mineralogical methods. Madison, WI: American Society of Agronomy; (1986): 1089-1102.
12. van Bochove E, N. Bertrand, J. Caron . In situ estimation of the gaseous nitrous oxide diffusion coefficient in a sandy loam soil. Soil Sci. Soc. Am. J. 62: 1178-1184; (1998).
13. Millington R. J., J. P. Quirk. Transport in porous media. In FA Van Beren et al., eds.Trans. Int. Congr. Soil Sci. 7th Vol. 1. Madison WI: Elsevier; (1960): 97-106.
14. Moldrup P., T. Olesen, J. Gamst, P. Schjønning , T. Yamaguchi, D.E. Rolston, Predicting the gas diffusion coefficient in repacked soil. Soil Sci. Soc. Am. J. 64: 1588-1594; (2000).
15. Marshall T. J., The diffusion of gases through soils. Soil Sci. 161: 79-82; (1959).
16. Moldrup P., T. Olesen, P. Schjønning, T. Yamaguchi, D.E. Rolston. Predicting the gas diffusion coefficient in undisturbed soil from soil water characteristics. Soil Sci. Soc. Am. J. 64: 94-100; (2000).

17. Moldrup, P., S. Yoshikawa, T. Olesen, T. Komatsu, D.E. Rolston, Gas diffusivity in undisturbed volcanic ash soils. Soil Sci. Soc. Am. J. 67: 41-51; (2003).
18. Campbell, G. S., A simple method for determining unsaturated conductivity from moisture retention data. Soil Sci. 117:311-314; (1974).
19. American Society for Testing and Materials (ASTM). Test methods for capillary-moisture relationships for course- and medium-textured soils by pressure plate apparatus, ASTM D 2325-68. In: 1987 Annual Book of ASTM Standards Vol. 04.08. Philadelphia PA: ASTM; (1987).
20. Rawlins S.L., G.S. Campbell. Water potential: Thermocouple psychrometry. In: Klute A, ed. Methods of soil analysis, Part 1, Physical and mineralogical methods. Madison, WI: American Society of Agronomy; (1986): 597-617.
21. Saltelli, A. S. Tarantola, F. Campologo, M. Ratto, Sensitivity analysis in practice: A guide to assessing scientific models. New York, NY: John Wiley & Sons; (2004).
22. Morris, M. D., Factorial sampling plans for preliminary computational experiments. Technometrics 33: 161-174; (1991).
23. Saltelli, A., K. Chan, E.M. Scott, Sensitivity Analysis. New York, NY: John Wiley and Sons; (2000).
24. Saltelli, A, S. Tarantola, K.Chan, A quantitative model-independent method for global sensitivity analysis of model output. Technometrics 41: 39-57; (1999).

Document No. DOE/NV/25946--081